

## Collision induced cluster fragmentation: From fragment size distributions to the caloric curve

B. Farizon, M. Farizon, M.J. Gaillard, F. Gobet, J.P. Buchet, M. Carré, P. Scheier, T.D. Märk

► **To cite this version:**

B. Farizon, M. Farizon, M.J. Gaillard, F. Gobet, J.P. Buchet, et al.. Collision induced cluster fragmentation: From fragment size distributions to the caloric curve. 5th International Symposium on Swift Heavy Ions in Matter SHIM 2002, May 2002, Taormina, Italy. pp.9-18, 10.1016/S0168-583X(02)02011-6 . in2p3-00013670

**HAL Id: in2p3-00013670**

**<http://hal.in2p3.fr/in2p3-00013670>**

Submitted on 12 Dec 2003

**HAL** is a multi-disciplinary open access archive for the deposit and dissemination of scientific research documents, whether they are published or not. The documents may come from teaching and research institutions in France or abroad, or from public or private research centers.

L'archive ouverte pluridisciplinaire **HAL**, est destinée au dépôt et à la diffusion de documents scientifiques de niveau recherche, publiés ou non, émanant des établissements d'enseignement et de recherche français ou étrangers, des laboratoires publics ou privés.

# Collision Induced Cluster Fragmentation: From Fragment Size Distributions to the Caloric Curve

**B. Farizon, M. Farizon, M.J. Gaillard, F. Gobet**

Institut de Physique Nucléaire de Lyon, IN2P3-CNRS et Université Lyon I  
43, boulevard du 11 novembre 1918, F-69622 Villeurbanne Cedex, France

**J.P. Buchet, M. Carré**

Laboratoire de Spectrométrie Ionique et Moléculaire, CNRS et Université Lyon I  
43, boulevard du 11 Novembre 1918, F-69622 Villeurbanne Cedex, France

**P. Scheier, and T.D. Märk,**

Institut für Ionenphysik, Leopold Franzens Universität, Technikerstr.25,  
A-6020 Innsbruck, Austria

## Abstract

We report on a cluster fragmentation study involving collisions of high-energy (60 keV/amu)  $H_3^+(H_2)_m$  hydrogen cluster ions ( $m=9,11$ ) with atomic helium or fullerenes. The experimental characterisation of the cluster fragmentation not only by the average fragment size distribution but also by a statistical analysis of the fragmentation events has become possible owing to a recently developed multi-coincidence technique in which all the fragments of all collisions occurring in the experiment are mass analysed on an event-by-event basis. By selecting specific decay reactions we can start after the energising collision with a microcanonical cluster ion ensemble of fixed excitation energy. From the respective fragment distributions for these selected decay reactions we derive corresponding temperatures of the decaying cluster ions. The relation between this temperature and the excitation energy (caloric curve) exhibits the typical prerequisites of a first order phase transition in a finite system, in the present case signalling the transition from a bound cluster type situation to the free gas phase.

**Key words:** *phase transition, caloric curve, cluster fragmentation; PACS: 36.40 Ei*

## 1 Introduction

Fragmentation [1] plays an important role for a wide range of objects in science and technology, such as polymer, colloids, droplets, rocks ...and corresponding investigations are developing very rapidly in quite different areas such as subatomic particles, soft matter and materials science. In addition, fragmentation of atomic nuclei is likely to become an effective way of handling nuclear wastes. Despite intensive research in various fields of science and technology complete analysis and understanding of fragmentation has not yet been achieved. Nevertheless, there is the recognition that general features of this phenomenon are rather independent of the actual system and its underlying interaction forces. Thus it is highly desirable to be able to study a model system in as much detail as possible in order to arrive at sound conclusions which may be applied (and compared) to a larger range of objects. Clusters that are aggregates of atoms or molecules in the form of microscopic and sub-microscopic particles have revealed themselves to be an appropriate system. The hydrogen cluster ions are the simplest ionised molecular complexes that for decades have attracted experimental efforts to clarify their structure and properties [2]. A number of experiments suggest that their structure consists of a tightly bound  $\text{H}_3^+$  core ion solvated by more weakly bound  $\text{H}_2$  molecules that are symmetrically arranged in solvation shells about the core in striking difference to the structure of the neutral clusters. Recent quantum Monte Carlo simulation [3] and quantum chemical calculations [4] have investigated the effect of protonation of pure hydrogen clusters  $(\text{H}_2)_n$  at low temperature. It was shown that the added proton gets trapped as a very localised and strongly bound  $\text{H}_3^+$  impurity in the cluster core surrounded by stable shells of more spatially delocalised solvating  $\text{H}_2$  molecules.

For fragmentation phenomena a natural classification should involve the fragmentation size distribution. These fragment size distributions often show a structure that may depend on external control parameters like the available energy, the density of the system, etc. Thus, the researchers in many fields are confronted with the need to characterise the data in a meaningful way and to determine the dynamical processes that cause fragmentation. High-energy cluster-atom or cluster-cluster collision experiments in which all fragments produced in from a particular collision are detected in coincidence could provide valuable information to test the predictions of general models describing fragmentation phenomena. One of the great challenges in cluster physics in the last years was the identification and characterisation of critical behaviour and the observation of phase transitions, including solid-to-liquid-like and liquid-to-gas-like phase transitions. Since clusters are particles of finite size one is confronted with the general question of how to detect

and/or characterise such a transition in a finite system. It has been proposed that the phase transition in finite systems within the microcanonical ensemble [5,6] may be detected by a characteristic functional relationship between the temperature and the excitation energy, the so-called caloric curve, i.e. a first order phase transition should correspond to a negative branch for the heat capacity [7-9].

In a strict sense, sharp second order phase transitions can only occur in the thermodynamic limit that is critical singularities are only present for a system with a large number of particles [10]. In small systems such as two colliding nuclear or molecular systems fluctuations may wash out the signature of the phase transition [11] (see also [8]). Nevertheless, it has been demonstrated theoretically (see [11] and references therein) and also experimentally (see [12] and references therein) that finite systems may indeed exhibit a critical behaviour to be seen when studying inclusive fragment size distributions, scaled factorial moments, and anomalous fractal dimensions. However, recent work on the lattice gas model [8] demonstrates that a critical behaviour is compatible with a first order phase transition because of the finite size effects. As concluded by Gross and co-workers [6, 13] on the basis of extensive theoretical modelling the best signature, however, of a phase transition of first or second order in a finite system is the specific shape of the caloric curve (see [7,9]) or according to the theoretical work of Berry and co-workers [14-16], specific dependence of the thermodynamic temperature on the total energy in the system.

Pochodzalla et al. [17] were the first to determine experimentally a relation between the temperature of hot decaying nuclei resulting from Au + Au collisions at 600 MeV/amu and their excitation energy, the shape of this relation exhibiting the characteristic plateau expected for a phase transition. The validity of this first experimental observation of a caloric curve for a liquid-to-gas phase transition for nuclear systems (in particular the determination of the temperature) was later questioned [8] because following experiments arrived at different shapes (see [18] and [19] and references therein). On the other hand, Haberland and co-workers [20-22] reported the first experimental determination of a caloric curve for the solid-to-liquid like transition (melting) of a small cluster i.e., a sodium cluster consisting of 139 atoms [20]. A beam of cluster ions was generated with a canonical distribution of internal energy thus fixing the temperature. One cluster size was selected (thus switching to microcanonical system), irradiated by photons and the photofragmentation pattern (which can be related to the energy) was measured as a function of cluster temperature. Moreover, Bachelors et al. [23] reported recently a caloric curve for a free tin cluster distribution (without mass selection) employing a sensitive pyroelectric foil, the interpretation of their experiment

was, however, later questioned [24]. Very recently Schmidt et al. [25] extracted the caloric curve for  $\text{Na}_{139}^+$  from 100 K up to the temperature where the clusters are boiling and spontaneously emit atoms. Simultaneously, we were able to extract from a high energy molecular hydrogen cluster collision experiment data allowing us to derive the relation between the temperature and the excitation energy (caloric curve) for the  $\text{H}_{27}^+$  cluster ions. This relation exhibited also the typical prerequisites of a first order phase transition in a finite system, i.e. signalling the transition from a bound cluster to the gas phase [26].

In the present paper, we report on a cluster fragmentation study involving collisions of high-energy hydrogen cluster ions  $\text{H}_{21}^+$  and  $\text{H}_{25}^+$  with atomic helium or fullerenes in which all the fragments of all collisions occurring in the experiment are mass analysed on an event-by-event basis using a novel multi-coincidence technique. We compare the fragment size distributions obtained with atomic helium with those obtained with fullerenes. Moreover, among the energising collisions between 60 keV/amu ions with a helium target we select a microcanonical ensemble of cluster ions with a given energy (by selecting specific decay reactions from a host of possible decay channels) and determine from the (partial) fragment size distribution the corresponding temperature of the ensemble of decaying cluster ions. This experiment involves the complete event-by-event analysis of 11685 collisions using a recently developed [12,27] multi-coincidence technique for the simultaneous detection of the correlated, ionised and neutral, collision fragments thus allowing to obtain an experimental caloric curve for the transition from a bound cluster to the gas phase.

## 2 Experimental set-up

Mass selected hydrogen cluster ions with an energy of 60 keV/u are prepared in a high-energy cluster ion beam facility [28] consisting of a cryogenic cluster jet expansion source combined with a high performance electron ionizer and a two step ion accelerator (consisting of an electrostatic field and a RFQ post-accelerator). After momentum analysis by a magnetic sector field, the mass selected high energy projectile pulse (pulse length  $\sim 100$  ms, repetition frequency  $\sim 1$  Hz) consisting in the present study of  $\text{H}_3^+(\text{H}_2)_9$  /or  $\text{H}_3^+(\text{H}_2)_{11}$  cluster ions is crossed perpendicularly by a helium target beam effusing from a cylindrical capillary tube (see as example Fig.1) or by a  $\text{C}_{60}$  effusive beam produced by evaporation of pure  $\text{C}_{60}$  powder in a single-chamber molybdenum oven (at about  $675^\circ\text{C}$ ) [29]. Prior to this the ion beam is collimated by two apertures ensuring an angular dispersion of about  $\pm 0.8$  mrad. One meter behind this collision region the high-energy hydrogen collision products (neutral and

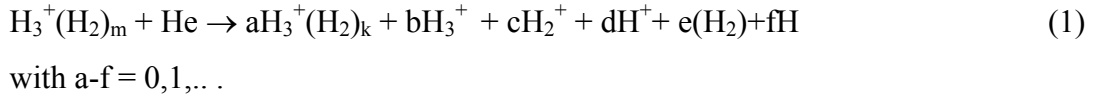
ionised) are passing a magnetic sector field analyser. The undissociated primary  $\text{H}_3^+(\text{H}_2)_{m=9}$  or  $11$  cluster projectile ion or the neutral and charged fragments resulting from reactive collisions are then detected approximately  $0.3 \mu\text{s}$  after the collision event with a multi-detector device consisting of an array of passivated implanted planar silicon surface barrier detectors located at different positions at the exit of the magnetic analyser.

With this instrument we are able to record for each event simultaneously the number (multiplicity) of each mass-identified fragment ion resulting from the interaction (for more experimental details, see [12, 29, 30]). In addition, for each event we can also monitor in coincidence with the detected ions the sum of the masses of all the neutral fragments. Moreover, by probing the angular distribution of these neutrals in front of the detector by using a movable aperture (0.5 mm of diameter) we find that the neutral products only consist of hydrogen atoms and hydrogen molecules [31] with no larger neutral clusters present. As example, we report in Figure 2a the spectrum corresponding to the detection of all the neutral fragments produced by collisions of  $\text{H}_{25}^+$  cluster ions with helium atoms without using the movable collimator. The number associated with each peak corresponds to the total neutral (mass number) for all the neutral fragments originating from one fragmented cluster ion  $\text{H}_{25}^+$ . We observe 15 separate peaks as described in reference [32]. In Figure 2b we show a spectrum obtained under the same experimental conditions but for this measurement the movable collimator is positioned in front of the detector for the neutral fragments. In this case the spectrum observed comprises only two major peaks at mass number 1 and 2 corresponding to the detection of H or  $\text{H}_2$  neutral fragments. Therefore, the different peaks observed at higher masses in Fig 2a correspond to the detection of several molecules and atoms for one event (spread out over a larger angle of incidence) and not to one neutral fragment of larger size (which should be equally well detected even with the collimator moved in). We also observed in Figure 2b a few events corresponding to mass three and four. These peaks cannot be interpreted as being due to bound neutral fragments (e.g.,  $\text{H}_4$ ) The diameter of the aperture in the collimator has been chosen in such a way that the probability to detect simultaneously two fragments originating from the same fragmented cluster is small, but this probability cannot be reduced to zero and therefore the signal at mass 3 and 4 is due to these rare occasions where two or more fragments pass the collimator.

From additional measurements with the molecular projectiles  $\text{H}_2$  or  $\text{H}_3^+$  using a movable grid in front of the detector, we can distinguish whether a resulting signal at a mass of 2 amu is due to one hydrogen molecule or two hydrogen atoms [33,31]. For larger clusters this technique cannot be directly applied and therefore additional information on relative cross

sections for the various product channels needs to be used for a complete analysis of the neutral mass peak [31].

Thus we are able to analyse on an event by event basis the identity of all correlated fragments produced in a single collision event between the  $H_3^+(H_2)_m$  cluster ion and the He target atom, the fragmentation reactions having the general form



The validity of single collision conditions has been ascertained by measurements at different He target pressures and allows also to derive absolute cross sections for the occurrence of specific reaction channels (partial cross sections) (for details see [34]). This complete analysis allows us to go beyond the straightforward determination of *total* fragment size distributions as reported previously [29] and references therein), since we are able to generate for the first time *partial* fragment size distributions for selected decay reactions or classes of decay reactions.

### 3 Size distributions of the charged fragments

Figure 3 shows the fragment ion yield  $Y_p$  (i.e. number of each fragment ion  $H_p^+$  divided by the total number of fragment ions per reactive collision) versus the fragment size  $p$  ( $p=3$  to  $23$ , odd) resulting from the fragmentation of  $H_{25}^+$  colliding with helium or  $C_{60}$ . The fragmentation of  $H_{25}^+$  with the helium target leads to a U-shaped fragment distribution. This distribution is very different from the one obtained in low energy collision [35] where the yield of the fragment ions is observed to increase with the fragment size. Such a behaviour observed here in the right part of the size distributions has been usually interpreted in the frame of the evaporative ensemble model. A major feature of the size distribution obtained in high-energy cluster-atom collision is, however, the prominent production of fragments with sizes in the “intermediate” regime between  $3 \leq p \leq 13$ .

In high-energy cluster-cluster collision, the fragmentation of  $H_{25}^+$  clusters exhibits a monotonously decreasing distribution, which is typical for the Intermediate Mass Fragment (IMF) case known in nuclear physics. This increase of the ion yield at the higher  $p$  values present in the helium target case is not observed in collisions with  $C_{60}$ . This can be interpreted from the relative probability of the different energy deposition that results from a collision.

Indeed, on average, small charged fragments are due to the violent collisions involving a large amount of energy transfer and large fragments are due to the more gentle type of interactions.

Most importantly, as can be seen in a log-log plot of these data in Fig.4, both the entire  $C_{60} - Y_p$  distribution and the left part of the He- $Y_p$  one ( $p/n \leq 0.5$ ) follow a power law  $p^{-\tau}$  yielding a  $\tau$  of 2.56 when fitting all the data (various size of clusters and various targets). Even more important, however, is that the present power law dependence is very similar to the IMF case in nuclear collision where the mass distribution follows a power law falloff with a  $\tau$  value of equal to 2.6 [36]. Moreover, there exists a strong similarity between the fragment size distribution and the predictions of certain models describing critical phenomena. The most famous is the Fisher droplet model [37] that allows calculate the droplet size distribution in a vapour. At the critical temperature the resulting distribution  $f(p)$  in sizes  $p$  is proportional to  $p^{-\tau}$  and the predicted exponent of 2.23 is close to the values observed for nuclear [36,38] and cluster fragmentation [28,29,39-41]. These cluster collision experiments around the Bohr energy (see [29] and references therein) have shown the formation of many different fragments in the exit channel of the reaction exhibiting a power law in total fragment size distributions. Such a power law, as described by the Fisher droplet model [37] is expected to hold for droplet condensation/evaporation near the critical temperature, indicating a liquid-to-gas second order phase transition.

To go one step further in the statistical analysis of the data obtained with energising collisions between 60 keV/amu ions with a helium target we can select a microcanonical ensemble of cluster ions with a given energy (by selecting specific decay reactions from a host of possible decay channels) and determine from the (partial) fragment size distribution the corresponding temperature of the ensemble of decaying cluster ions. In the following part, we show as an example, the data obtained for  $H_{21}^+$  cluster ions.

#### **4 Construction of a caloric curve**

As we need for the construction of a caloric curve the simultaneous determination of the energy and the temperature of the system, we use the ability to select certain classes of reactions and to group our analysed events into a number of different subgroups each representing collisions in which a certain amount of energy is deposited into the cluster. Thus we are generating from our large set of collisions various subsets containing only cluster ions with a certain energy (or energy range) in a microcanonical sense. The basic idea behind this is to analyse each decay reaction in terms of the energy required for all the particles produced

in such a decay reaction (taking into account the well known potential energy curves for the hydrogen molecule when calculating the energy for the Franck-Condon transitions from quasi-isolated cold ground state  $H_2$  molecules to the various excited states involved) and to use the total energy value obtained as a measure for the internal energy prior to the decay. For instance, analysing the identity of the neutrals in the observed decay reactions of  $H_3^+(H_2)_{m=9}$  ion into  $H_9^+ + H_2^+$  plus a neutral mass totalling 10 amu shows that xxx% of the cases correspond to the production of five hydrogen molecules. In this case the necessary energy for the reaction is 15.7 eV (the ionisation energy for the hydrogen molecule) neglecting the much smaller binding energy of the hydrogen molecules. Similarly, xxx% of these events correspond to the production of four hydrogen molecules and two hydrogen atoms necessitating an additional energy input of about 10.3 eV to dissociate one molecule into two atoms (thus yielding a total energy of 26 eV), xxx% correspond to three molecules and four atoms (total energy of 36.3 eV) and xxx% to two molecules and six atoms (total energy of 46.6 eV).

Fig.5 shows for the  $H_3^+(H_2)_{m=9}$  cluster ion projectile the corresponding measured partial fragment mass distribution for eight selected subsets each of which includes reactions of a certain energy range, e.g., 2-12 eV, 15-25 eV, etc. It is interesting to note that the shape of these distributions changes significantly as a function of the energy deposited, i.e., from a U-shaped form at low energy which is due to the occurrence of a mixture of evaporation and multi-fragmentation processes, to a pure power law at intermediate energies due to the presence of only multi-fragmentation reactions to finally a regime at high energies which is dominated by complete disintegration processes. So far these different regimes could only be observed by different experiments with widely different collision parameters ranging from low energy mass spectrometer collision experiments [35], to high-energy cluster/atom or nuclear collision experiments (see [29] and references therein) and to beam foil experiments with clusters yielding only atomic fragment ions [43]. This is the first time (see also results given for the  $H_{27}^+$  [26] and for the  $H_{25}^+$  [42]) that this characteristic change of the mass distribution as a function of energy deposited has been determined in only one experiment over the whole range of possible shapes and thus possible decay mechanisms.

Returning now to the construction of the caloric curve we need in a second step to determine for each subset of known energy the corresponding temperature of the cluster ions prior to the decay. Here we use a relationship between the characteristic shape of a fragment mass distribution and the temperature of the decaying nuclei at around the critical point reported recently by Belkacem et al. [11]. They were able to fit quite differing numerical mass

distributions obtained by classical MD calculations for an A=100 nucleus at different initial canonical temperatures (by generating 2000 events per temperature) very well with Fisher's droplet formula [37]

$$dN/dA = Y_0 A^{-\tau} X^{A^{2/3}} Y^A \quad (2)$$

with  $Y_0$ ,  $X$ ,  $Y$  and  $\tau$  fitting parameters and  $A$  the atomic mass number, thus demonstrating a direct relationship between the shape of the mass distribution (as described by (2) and in particular by the parameter  $Y$  which is related to the temperature approaching the value 1 at the critical temperature) and the initial temperature of the decaying system (see also [44]). In reference [11] mass distributions are reported obtained in the expansion of the system A=100 with eight different initial temperatures ranging from 2 to 20 MeV showing a similar evolution of the fragment size distribution as observed with increasing degree of excitation in Fig. 5.

Following the methodology of Belkacem et al [11] in fitting their mass distribution, i.e., first fixing the parameter  $\tau$  using a rather pure power law distribution (e.g., the one at an energy of 47 eV in Fig.5) and then fitting the other parameters by using all distributions (and doing this in an iterative way several times), we also fitted the presently obtained (partial) fragment mass distributions with formula (2). With a slope of  $-3.22$  (as compared to  $-2.23$  in the calculation of Belkacem et al [11]; previous experimentally determined values for total fragment mass distribution for clusters and nuclei having values of about  $-2.6$  [45]) we obtain a very good agreement between the experimental points and the fits shown in Fig.5 by solid lines. In the case of the  $H_3^+(H_2)_{m=12}$  [26] we used a slope of  $-3.38$  and the fits obtained were equally convincing. This then allows us by comparison with the results of Belkacem et al [11] to designate for each of the subsets considered a relative measure for the temperature due to the characteristic shape of its fragment mass distribution (as expressed by the fitted parameters, in particular the parameter  $Y$ ). It has to be noted that in the cluster case we observe a small increase of  $N(p)$  for the highest fragment sizes (see the distribution corresponding to the energy [55-65] eV). This is not observed in the distributions reported by Bonasera and co-workers [11]. By using the fit of Fisher this effect is attenuated. One of the important points will be to develop a fitting function other than the Fisher law allowing to take into account this effect.

The overriding conclusion from these results is that for small energies the distribution is quickly changing with increasing energy from a U-shaped form to a single power law fall off. Moreover, this power law containing fragments of all sizes is sustained over a broad energy range and thus this is direct evidence for a constant temperature in this energy range. Finally, at very large energies this power law is replaced by a shape, which is falling off much faster than this power law signalling a sudden change (increase) in temperature. It is interesting to note that in a similar fashion, though in a different context and by different theoretical means, temperatures of decaying carbon cluster ions have been determined by measuring either the microcanonical decay rate constants for monomer evaporation [46] (see also results for aniline-argon clusters [47], the kinetic energy release distributions for monomer evaporation [48] or the fragmentation pattern in surface-induced dissociations [49]). Using this « temperature » which is only a relative measure (due to the comparison with MD calculations applied to the nuclear matter), we plot in Fig.6 the temperature derived in reduced units versus the energy deposited. As a matter of fact we have for this purpose considered more data subsets than shown in Fig.5. Moreover, similar results have also been obtained for other cluster ions as shown in reference [26, 42] thus confirming independence of this characteristic result from the finite particle size.

## 5 Conclusion

This caloric curve shown in Fig.6 can be clearly divided into three parts, after an initially increase, a distinct plateau is present before the curve is rising again. This curve therefore agrees qualitatively with the typical prerequisites of a first order phase transition [6] in a finite system. It thus constitutes a strong signature for a liquid-to-gas like phase transition in a fragmenting cluster and thus confirms and replaces the other fingerprints such as the power law in mass distributions and factorial moment analyses [13]. As in the calculations discussed by Gross et al. using microcanonical metropolis sampling for hot atomic metal clusters the transition occurs and is characterised by the interplay and transition from monomer evaporation reactions (see also Fig.4), to multi-fragmentation reactions and complete vaporisation events in this bound-free transition regime. The particular long plateau, also observed for sodium cluster ions [25], may be attributed to the many different degrees of freedom available in this special type of cluster being bound by a mixture of dispersion forces (intermolecular binding) and covalent binding with more intramolecular excited states available than in atomic clusters.

## *Acknowledgements*

*Work supported by the FWF, Wien, Austria, the Amadee program of the French and Austrian governments and the EU Commission, Brussels.*

## References

1. D. Beyson, X. Campi, E. Pefferkorn (eds), *Fragmentation Phenomena* (World Scientific, Singapore, 1995).
2. I. Stich, D. Marx, M. Parrinello, K. Terakura, J. Chem. Phys. 107, 9482 (1997).
3. I. Stich, D. Marx, M. Parrinello, K. Terakura, Phys. Rev. Lett. 78, 3699 (1997).
4. M. Farizon, H. Chermette, and B. Farizon-Mazuy, J. Chem. Phys. 96, 1325 (1992).
- 5 - W. Thirring, Z. Phys. 235, 339 (1970).
- 6 – D.H.E.Gross Physics Reports 279 (1997) 119-201 and references therein.
- 7 – P. Chomaz and F. Gulminelli, Phys. Rev. Lett., 85 (2000) 3587
- 8 - F. Gulminelli and P. Chomaz, Phys. Rev. Lett., 82 (1999) 1402.
- 9 - P. Chomaz et al., proceedings of theXXXVIII International Winter Meeting on Nuclear Physics, Ricerca Scientifica ed Educazione Permanente supplemento, n°116, (2000) p336
- 10 - P. Chomaz and F. Gulminelli, Nucl. Phys., A647 (1999) 153.
- 11 - M.Belkacem et al., Phys. Rev., C52 (1995) 271.
- 12 - B.Farizon et al., Phys. Rev. Letters, 81 (1998) 4108.
- 13 - A.S.Botvina and D.H.E.Gross, Phys. Letters, B408 (1997) 31.
- 14 - D.J.Wales and R.S.Berry, Phys. Rev. Lett., 73, (1994) 2875.
- 15 - A. Proykova and R.S.Berry, Z. Phys., D40 (1997) 215.
- 16 - R.E.Kunz and R.S.Berry, Phys. Rev. E49 (1994) 1895.
- 17 - J.Pochodzolla et al., Phys. Rev. Lett., 75 (1995) 1040.
- 18 - Y.G.Ma et al., Phys. Letters, B390 (1997) 41.
- 19 - M.D'Agostino et al., Nucl. Phys., A650 (1999) 329.
- 20 - M.Schmidt et al., Phys. Rev. Lett., 79 ,(1997) 99.
- 21 - M.Schmidt et al.,Nature, 393 (1998) 238
- 22 - R.Kusche et al., Eur. Phys. J., D9 (2000) 1
- 23 - T.Bachels et al., Phys. Rev. Lett., 85 (2000) 1250
- 24 - K.Kofman et al., Phys.Rev. Lett., 86 (2001) 1388
- 25 - M. Schmidt et al., Phys. Rev. Lett , 033146 (2001)
- 26 – F. Gobet et al., Phys. Rev. Lett, 028146 (2001)
- 27- B.Farizon et al., Phys. Rev. B60 (1999) 3821.

- 28 B. Farizon, M. Farizon, M.J. Gaillard, E. Gerlic, S. Ouaskit, *Conference on polyatomic impact on solids and related phenomena, St Malo Juin 1993*, Nucl. Instr. and Meth. in Phys. Res. B **88**, 86 (1994).
- 29 - B.Farizon et al., Int. J. Mass Spectrom. Ion Proc., 164 (1997) 225.
- 30 - B.Farizon et al., Eur. Phys. J. D 5 (1999) 5.
- 31- See F.Gobet, Thèse de doctorat, Université Lyon 1, 2001, where we discuss in detail the analysis of the neutral fragments, i.e., by probing the angular distribution of the neutrals in front of the detector using a movable collimator.
- 32 – B. Farizon et al., Int. J. Mass Spectrom. Ion Proc., 144 (1995) 79.
- 33 - G.Jalbert et al., Phys. Rev.,A47 (1993) 4768
- 34 - B.Farizon et al., Nucl. Instr. Meth. Phys. Res., B101 (1995) 287.
- 35 - A.Van Lumig and J.Reuss, Int. J. Mass Spectrom. Ion Phys., 27 (1978) 197.
36. X. Campi, Nucl. Phys. A **495**, 259c (1989).
- 37 - M.E.Fisher, Rep. Progr. Phys., 30 (1967) 615.
- 38 A. Hirsch et al, Phys.Rev. C **29**, 508 (1984).
39. T. LeBrun et al, Phys. Rev. Lett. **72**, 3965 (1994).
40. J. Schulte, Phys. Rev. B **51**, 3331 (1995).
41. P. Scheier et al, Int. Rev. Phys. Chem. **15**, 93 (1996).
- 42 B. Farizon et al., Int. J. Mass Spectrom. Ion Proc., to be published (2002)
- 43 - B.Mazuy et al., Nucl. Instrum. Meth., B28 (1987) 497.
- 44 - V.N.Kondratyev and H.O.Lutz, Z. Phys., D40 (1997) 210.
- 45 - J.E.Finn et al. , Phys. Rev. Letters, 49 (1982) 1321.
- 46 - H.Hohmann et al., Z. Phys., D33 (1995) 143.
- 47 - P.Parneix et al., Chem. Phys., 239 (1998) 121.
- 48 - S.Matt et al., J. Chem. Phys., 113 (2000) 616.
- 49 - T.Fiegele et al., Chem. Phys. Lett., 316 (2000) 387

## Figure Headings.

### Fig.1

Schematic view of the experimental set-up. Mass selected hydrogen cluster ions of 60 keV/amu energy are crossed perpendicularly by an helium gas jet (or an effusive C<sub>60</sub> beam) in the collision region. Neutral and charged hydrogen fragments are passing through a magnetic sector field analyser one meter behind this collision region and then are detected in coincidence with a multi-detector device consisting of a number of surface-barrier detectors

located at different positions at the exit of the analyser. For each fragmented cluster, the size and the number of the different fragments are recorded allowing a statistical analysis as presented in the following.

### **Fig.2**

Mass spectrum for neutral fragments for decaying  $H_{25}^+$ : a) without movable collimator in front of the detector b) with movable collimator in front of the detector

### **Fig3**

Normalized fragment ion yield  $Y_p$  versus normalized fragment size  $p/25$  for  $H_{25}^+$  cluster ions interacting at 1.5 MeV collision energy with a helium or a  $C_{60}$  target, respectively.

### **Fig.4**

Log-Log plot of normalized fragment ion distributions for  $H_{25}^+$  cluster ions interacting at 1.5 MeV collision energy with a helium or a  $C_{60}$  target, respectively.

### **Fig. 5**

Partial fragment mass distributions for different subsets of reaction channels (selected according to the energy deposited in the collision complex, i.e; 2-12 eV, 15-25 eV, etc.) occurring in collisions of 60 keV/amu  $H_{21}^+$  ions with He. Solid lines: fits using Fisher's formula (see text).

### **Fig. 6**

Caloric curve for cluster fragmentation: temperature (given in reduced value  $(T/T_0)$  with  $T_0$  the temperature in the plateau part of the curve versus the energy deposited in the  $H_{21}^+$  cluster ion. The error bar given for one of the experimental points comprises, on the one hand, the maximum error in assigning the energy including the unknown extent of vibrational excitation in the one hydrogen molecule hit on average by the He atom during the collision and, on the other hand, the maximum error in assigning the temperature using various fitting procedures. In practice as we are using the best fit method for all the points the relative error in the temperature is much smaller and this is also mirrored by the rather small deviations of the experimental points from each other in the plateau region. This interpretation is confirmed by similar observations for other cluster sizes.